Sample-dependent and sample-independent thermal transport properties of α-$RuCl_3$

Heda Zhang,[1] Andrew F. May,[1] Hu Miao,[1] Brian C. Sales,[1] David G. Mandrus,[1] Stephen E. Nagler,[2] Michael A. McGuire,[1] and Jiaqiang Yan[1,*]

[1]*Materials Science and Technology Division, Oak Ridge National Laboratory, Oak Ridge, Tennessee 37831, USA*
[2]*Neutron Scattering Division, Oak Ridge National Laboratory, Oak Ridge, Tennessee 37831, USA*

(Received 28 March 2023; revised 14 June 2023; accepted 18 October 2023; published 13 November 2023)

We investigated the thermal transport properties of two α-$RuCl_3$ crystals with different degrees of stacking disorder to understand the origin of the previously reported oscillatory feature in the field dependence of thermal conductivity. Crystal I shows only one magnetic order around 13 K, which is near the highest T_N for α-$RuCl_3$ with stacking faults. Crystal II has less stacking disorder, with a dominant heat capacity at 7.6 K along with weak anomalies at 10 and 13 K. In the temperature and field dependence of thermal conductivity, no obvious anomaly was observed to be associated with the magnetic order around 13 K for either crystal or around 10 K for crystal II. Crystal II showed clear oscillations in the field dependence of thermal conductivity, while crystal I did not. For crystal I, an L-shaped region in the temperature-field space was observed where thermal Hall conductivity κ_{xy}/T is within ±20% of the half quantized thermal Hall conductivity κ_{HQ}/T, while for crystal II, κ_{xy}/T reaches κ_{HQ}/T only in the high field and high temperature regime with no indication of a plateau at κ_{HQ}/T. Our thermal conductivity data suggest the oscillatory features are inherent to the zigzag ordered phase with T_N near 7 K. Our planar thermal Hall effect measurements suggest the sensitivity of this phenomena to stacking disorder. Overall, our results highlight the importance of understanding and controlling crystallographic disorder for obtaining and interpreting intrinsic thermal transport properties in α-$RuCl_3$.

DOI: 10.1103/PhysRevMaterials.7.114403

I. INTRODUCTION

In the last decade, α-$RuCl_3$ was intensively studied as a promising candidate material for realizing Kitaev quantum spin liquids that have Majorana fermions as the elementary excitation [1]. α-$RuCl_3$ is a cleavable, layered magnetic material with the van der Waals bonded honeycomb layers formed by edge sharing $RuCl_6$ octahedra [2]. Below $T_N \approx 7$ K, α-$RuCl_3$ shows a zigzag type magnetic order [3]. However, this magnetic order can be suppressed by applying an in-plane magnetic field above ≈7 T. A field-induced quantum spin liquid state is proposed in the intermediate field range before getting to the field polarized state at even higher fields. Recently, there are two fascinating observations on the thermal transport properties of α-$RuCl_3$ in the field-induced quantum spin liquid state. The first one is the observed half-integer quantized thermal Hall conductance which is believed to be one of the fingerprints for Majorana fermions of the fractionalized spin excitations in α-$RuCl_3$ [4]. While some groups reported the plateaulike feature at half quantized value in a certain temperature and field range, other groups observed a strongly temperature-dependent thermal Hall conductance and proposed a bosonic origin of the observed thermal Hall effect [5–10]. The other intriguing experimental observation is the oscillatory features of the longitudinal thermal conductivity as a function of in-plane magnetic field [11]. These oscillations were reproduced by different groups [12,13] but the origin is under hot debate. Czajka *et al.* proposed the observed oscillations as quantum oscillations of putative charge-neutral fermions akin to those produced by Landau quantization of electron states in a metal in the presence of magnetic fields [11], while others believed that the observed oscillatory features are the result of a sequence of magnetic field-induced magnetic phase transitions [12–14]. The experimental observation and understanding of the underlying physics are under debate for these two fascinating thermal transport properties, partially due to the materials issue of α-$RuCl_3$ [15].

Due to the weak van der Waals bonding between the honeycomb layers, α-$RuCl_3$ crystals are susceptible to stacking disorder that can form during crystal growth and sample handling. Regardless of the origin, stacking faults affect the physical properties [16–18]. As demonstrated before [19], mechanical deformation can lead to magnetic anomalies in the temperature range 7–14 K. This property makes possible a comparative study of thermal transport properties of α-$RuCl_3$ crystals with different amount/distribution of stacking disorder. In particular, this might lead to a control of the oscillatory features if they are indeed due to the field-induced magnetic phase transitions.

Motivated by this, we investigated the thermal transport properties of α-$RuCl_3$ with different amounts of stacking disorder introduced by mechanical deformation. Results from two crystals are presented in this paper. Crystal I shows a high Néel temperature near 13 K. Crystal II has less stacking disorder and shows two weak anomalies near 10 and 13 K in addition to a dominant peak near 7.6 K in the temperature

*yanj@ornl.gov

dependence of specific heat. For both crystals, no obvious anomaly in the temperature and field dependence of thermal conductivity was observed to be associated with the magnetic order around 13 or 10 K. Our results suggest that the oscillatory features of thermal conductivity should be innately tied to the zigzag ordered phase with T_N around 7 K. This observation is at odds with the idea that the magnetic transitions at, for example, 10 and 13 K can contribute to the oscillatory features in α-$RuCl_3$. Quite different planar thermal Hall effect was observed for those two crystals studied in this work. Overall, this work highlights the importance of controlling stacking disorder for more intrinsic thermal transport properties of α-$RuCl_3$.

II. EXPERIMENTAL DETAILS

Millimeter-sized α-$RuCl_3$ crystals were grown using the conventional vapor transport technique with a temperature gradient of 250 °C along the growth ampoule. About 0.3 g of α-$RuCl_3$ powder synthesized by reacting RuO_2 powder with $AlCl_3$-KCl salt [20] was sealed under vacuum inside of a fused quartz tube with an outer diameter of 16 mm, a wall thickness of 1.0 mm, and a length of 200 mm. The sealed ampoule was put inside of a two-zone tube furnace. The hot end with the starting powder was kept at 1000 °C and the cold end at 750 °C. After a week, the furnace was powered off to cool to room temperature. This kind of vapor transport growth results in platelike crystals with in-plane dimension up to 4–5 mm and thickness up to 0.2 mm. Similar sized single crystals could also be obtained using a self-selecting vapor transport technique [21] when a cooling rate higher than 20 °C/h is used.

Magnetic properties were measured with a Quantum Design (QD) magnetic property measurement system in the temperature range $2.0\,\text{K} \leqslant T \leqslant 30$ K. Specific heat data below 30 K were collected using a QD physical property measurement system (PPMS). Magnetic property and specific heat measurements confirm the as-grown crystals have only one single magnetic transition with the ordering temperature, T_N, of 7.6 K. The well-characterized crystals were then attached to kapton tape and the thickness was adjusted by peeling off part of the crystal with scotch tape. The kapton tape was then bent a couple of times to introduce stacking fault to the adhered α-$RuCl_3$ crystals. This approach allows us to introduce stacking disorder without crumpling the crystals. As reported before [19], the stacking fault introduced this way will result in secondary magnetic phases with T_N in the temperature range 7.6–14 K. Intermediate magnetic measurements were performed during the bending process to monitor the anomalies in the temperature dependence of magnetization. In the end, the kapton tape was carefully removed.

Thermal transport measurements were carried out on a custom-built PPMS puck. We use Cernox temperature sensors, and Model 336 cryogenic temperature controllers as thermometers. A 1 kΩ resistor was used as the heater. We use gold wires (25 μm) for thermal contact and manganin wires (25 μm) for electric contact while minimizing thermal leakage. Contacts were made using silver paint from DuPont. All thermal transport measurements were carried out under high vacuum. The temperature dependence of magnetic susceptibility and specific heat below 20 K was measured before and after measuring the thermal transport properties. This is to confirm that the thermal transport measurement does not introduce observable change to the magnetic properties and specific heat. It should be mentioned that magnetization, specific heat, and thermal transport properties for each type of crystals are all measured on exactly the same piece of crystal.

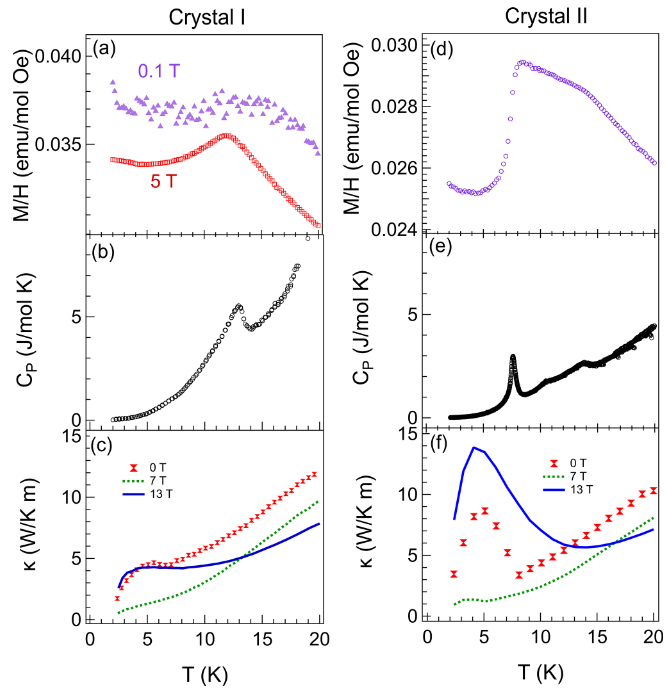

FIG. 1. Magnetization, specific heat, and thermal conductivity of (a)–(c) crystal I and (d)–(f) crystal II below 20 K. (a) Temperature dependence of magnetization of crystal I measured with magnetic field applied along the zigzag direction (perpendicular to the Ru-Ru bond). The magnetic data collected in a field of 0.1 T is noisy because the crystal is only 0.15 mg. We thus also show the data collected in a field of 5 T that leads to a slightly lower T_N [12,18]. (b) Specific heat of crystal I showing a dominant λ-type anomaly around 13 K and a very weak anomaly barely observable near 7 K. (c) Thermal conductivity of crystal I measured in different magnetic fields. (d) Temperature dependence of magnetization of crystal II showing two anomalies at 7 and 14 K. The data were collected in a magnetic field of 0.1 T applied along the zigzag direction. (e) Specific heat of crystal II showing a dominant λ-type anomaly at 7.6 K and two weak anomalies around 10 and 14 K. Specific heat data for both samples were collected in zero magnetic field. (f) Thermal conductivity of crystal II measured in different magnetic fields. Both the heat current and magnetic field are along the zigzag direction.

III. RESULTS AND DISCUSSION

Figure 1 shows the temperature dependence of magnetization, specific heat, and thermal conductivity below 20 K for two different crystals. From the magnetization and specific heat data shown in Figs. 1(a) and 1(b), crystal I shows a magnetic order at $T_N = 13$ K. A weak feature barely observable near 7 K in Fig. 1(b) indicates the presence of a small fraction of the original nondeformed phase. Crystal II has a smaller amount of stacking fault and three anomalies can be observed in the specific heat data shown in Fig. 1(e). The dominant one is found at 7.6 K and two weaker anomalies are found around 10 and 13 K. These two crystals enable us to investigate how the stacking disorder affects the thermal transport properties. We tried to obtain a crystal with only one magnetic order with T_N around 10 K but failed.

The response of longitudinal thermal conductivity of α-$RuCl_3$ to the zigzag magnetic order has been reported by many groups [9,22–25]. Despite the variation of the magnitude, the thermal conductivity data reported by different groups show similar temperature dependence: Thermal conductivity is enhanced upon cooling through T_N and shows a peak at around 5 K. This kind of recovery of lattice thermal conductivity upon cooling through a magnetic order has been observed in many other systems with strong spin-lattice coupling. From a simple analogy, one would expect thermal conductivity to resurge upon cooling below 13 K for crystal I and show some weak anomalies near 10 and 13 K for crystal II. Figures 1(c) and 1(f) show the temperature dependence of thermal conductivity of both crystals. Surprisingly, no obvious anomaly was observed above 7.6 K in zero magnetic field. Both crystals show a recovering of thermal conductivity when cooling below 7.6 K. This feature is much more dramatic for crystal II than that for crystal I. Around 5 K where the thermal conductivity peaks, the thermal conductivity of crystal II is about twice that for crystal I. This is consistent with the fact that crystal II has a much stronger response in magnetization and specific heat near T_N at 7.6 K. The absence of an observable anomaly around 13 K and the recovery upon cooling through 7.6 K for both crystals indicate that the magnetic order at 7.6 K has a more dramatic effect on the longitudinal thermal conductivity of α-$RuCl_3$. Despite a bulk behavior of the magnetic order at 13 K for crystal I as manifested by the well-defined anomalies in the temperature dependence of magnetization and specific heat, this magnetic order induces no observable anomaly around T_N in the temperature-dependent thermal conductivity. This interesting observation inspires us to study how the thermal conductivity responds to a high in-plane magnetic field.

Figures 1(c) and 1(f) also show the temperature-dependent longitudinal thermal conductivity measured in magnetic fields of 7 and 13 T applied along the zigzag direction (perpendicular to the Ru-Ru bond). In the spin-polarized state, crystal II shows a much higher thermal conductivity at low temperatures. This is consistent with the larger increase of thermal conductivity below T_N for crystal II when measured in zero magnetic field. In an applied magnetic field of 7 T, the long-range magnetic order is suppressed and so is the lattice heat transport. The temperature-dependent thermal conductivity data collected in high magnetic fields indicate that the applied magnetic field does not introduce extra anomalies around 10 or 13 K. This information is important when understanding whether the field-induced magnetic phase transitions would contribute to the oscillatory features in the field-dependent thermal conductivity.

Figure 2(a) shows the field dependence of thermal conductivity at low temperatures for both crystals. For crystal II, the oscillatory features can be well resolved. At 2 K, the minima in magnetothermal conductivity show up at 6.2, 7.5, 8.6, 9.6, and 11.2 T. As shown in Fig. S1 in the Supplemental

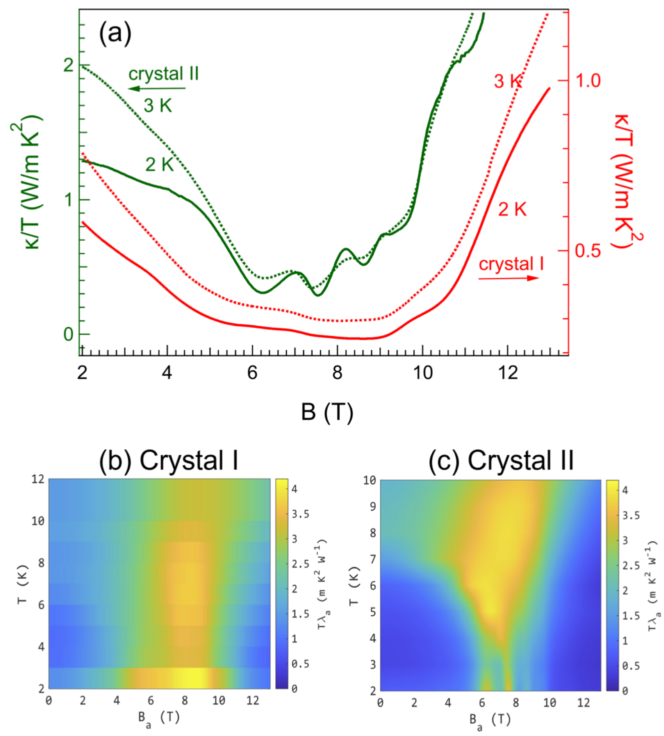

FIG. 2. Field dependence of longitudinal thermal conductivity κ_{xx}/T. (a) κ_{xx}/T at low temperatures. (b), (c) Color plot of κ_{xx}/T in the temperature-field space studied in this work. Both the heat current and the magnetic field are along the zigzag direction (or perpendicular to the Ru-Ru bond).

Material [26], the presence of the oscillatory features and the critical fields agree well with those observed in our α-$RuCl_3$ crystals with minimal amount of stacking disorder and also with those reported previously by other groups [11,12]. In contrast to the pronounced oscillating features for crystal II, only rather weak features are observed for crystal I in the magnetothermal conductivity curves in the field range of 4–12 T. These weak features follow the similar field dependence as for those oscillatory features for crystal II. This similar field dependence suggests for crystal I that (1) those weak features may come from the residual small fraction of the original phase with $T_N = 7.6$ K, and (2) the magnetothermal conductivity is also dominated by the $T_N = 7.6$ K phase and there are no unique features that could be attributed to those secondary magnetic phases with $T_N > 7.6$ K. This is quite different from our expectation. According to previous studies of the magnetic order in applied magnetic field [12,18], the $T_N = 13$ K magnetic order should be suppressed by an in-plane magnetic field near 9 T. Around this magnetic field, one would expect a well-defined feature in the magnetothermal conductivity curve of crystal I if the oscillatory features observed by different groups come from the field-induced phase transitions. Surprisingly, we did not observe any feature dominated by the magnetic phase with $T_N = 13$ K in our magnetothermal conductivity data for crystal I. Since the stacking disorder is introduced by bending the crystals after growth, one might wonder whether thermal conductivity responds to the stacking-induced magnetic orders with $T_N > 7.6$ K in a wider temperature and/or field

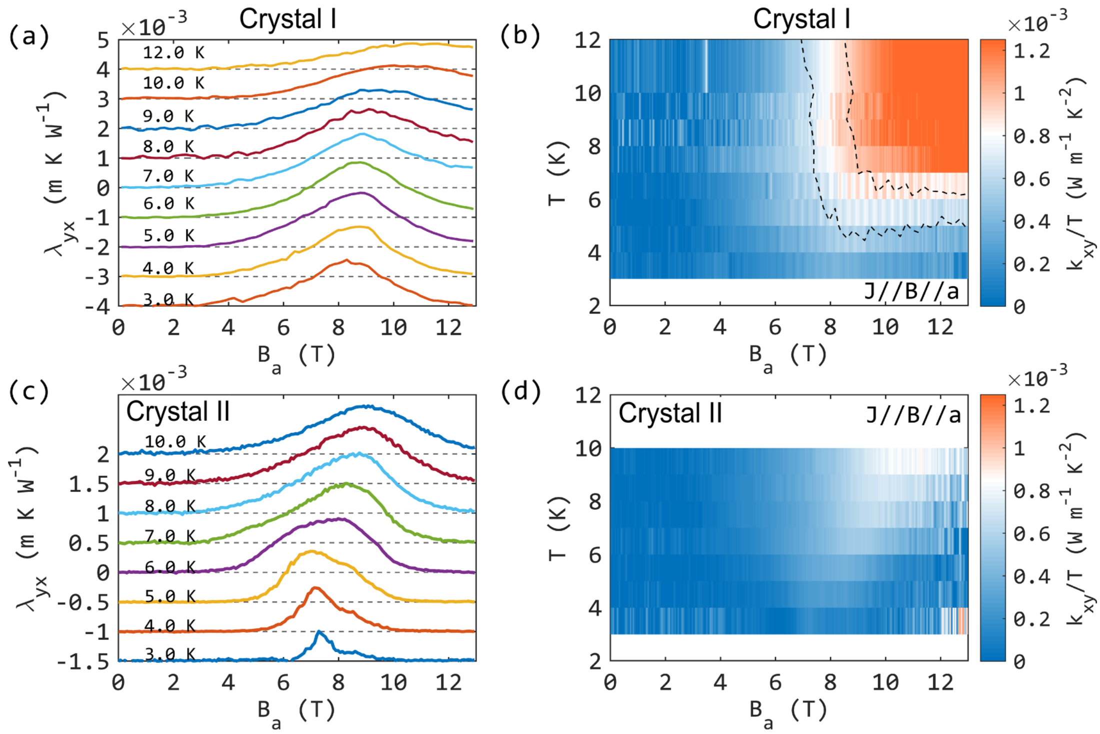

FIG. 3. Planar thermal Hall response with magnetic field and heat current parallel to the zigzag direction (or perpendicular to the Ru-Ru bond). (a), (c) Field dependence of thermal Hall resistivity at different temperatures for crystal I (a) and crystal II (c). The horizontal dashed lines show the zero baseline for each temperature. (b), (d) Color plot of thermal Hall conductivity κ_{xy}/T for crystal I (b) and crystal II (d). The dashed lines in (b) highlight the L-shaped region where the κ_{xy}/T is within $\pm 20\%$ of κ_{HQ}/T. The sample stage temperature is used here. As demonstrated in Fig. S3 in the Supplemental Material [26], the same feature is also observed when the thermal Hall conductivity is scaled by the sample temperature. The line plots of κ_{xy}/T data used in (b) and (d) are presented in Fig. S4 in the Supplemental Material [26].

range. If this is true, one does not expect to see well-defined features from field-induced phase transitions in the magnetothermal conductivity curves for crystal II. The absence of any recovery of lattice heat transport upon cooling across $T_N = 10$ or 13 K in zero magnetic field could also be explained by assuming that phonons are already seriously scattered by lattice defects in these phases. However, one would not expect any anomaly in magnetothermal conductivity when these magnetic orders are disrupted by external magnetic fields, because the applied magnetic fields can suppress the magnetic orders but cannot eliminate the lattice defects and their scattering to phonons.

Compared to crystal II, crystal I has a much smaller thermal conductivity due to the populated stacking disorder. However, the suppressed phonon heat transport by lattice defects should not be responsible for the suppressed oscillatory features. To verify this, we investigated the temperature and field dependence of thermal conductivity for a 2%-Ir doped crystal (see Fig. S2 in the Supplemental Material [26]). 2% Ir substitution at the Ru site slightly suppresses T_N but suppresses thermal conductivity to be comparable to that of our crystal I. Interestingly, oscillatory features can be well resolved in this 2%-Ir substituted sample although the magnitude becomes weaker.

Figures 2(b) and 2(c) show the color plot of thermal resistivity $T\lambda$ over the whole temperature-field space investigated in this work. The oscillatory features cannot be well resolved any more above 4 K for crystal II and the overall feature shown in Fig. 2(c) agrees well with what is reported by Czajka *et al.* [10]. For crystal I with the dominant magnetic order at 13 K, the weak anomalies observed at 2 K also disappear above 4 K and the field range, in which $T\lambda$ shows a maximum, exhibits little change with increasing temperature.

The above results suggest that the magnetic phases with $T_N = 10$ and 13 K do not produce observable signatures in thermal conductivity. However, our planar thermal Hall data suggest that they or the stacking disorder can have a significant effect on the thermal Hall effect of α-RuCl$_3$. Figures 3(a) and 3(c) show the field dependence of thermal Hall resistivity measured at different temperatures up to 12 K. For crystal I, a nonzero thermal Hall resistivity was observed in a wide field range of 4–12 T and a broad peak centering at around 8.5 T was observed at 3 K. This magnetic field is similar to that required to suppress the magnetic order at $T_N = 14$ K [12,18]. With increasing temperature, this broad peak moves toward higher magnetic field. For crystal II at 2 K, in addition to an anomaly at around 8.5 T, the dominant feature centers at around 7.2 T. The evolution with temperature of this dominant feature follows the change of T_N in applied magnetic field and cannot be well resolved above 8 K. Above 8 K, the feature around 8.5 T shows the same temperature dependence as the main feature for crystal I shown in (a). Around 6 K, these two features are comparable to each other and a plateau can be observed in the field dependence of thermal Hall resistivity. It is worth mentioning that the critical magnetic field of 7.2 T marks the threshold for transitioning from the zigzag ordered phase to the field-induced quantum spin liquid state, while the field of 8.5 T is similar to the threshold required for the crossover between the field-induced quantum spin liquid state and the partially polarized state for $RuCl_3$. Whether this observation indicates any strong correlation between the thermal Hall effect and the magnon gap change deserves further study. Figures 3(b) and 3(d) show the color plot of thermal Hall conductivity κ_{xy}/T. The dashed curves highlight the region where the κ_{xy}/T is within ±20% of the half quantized thermal Hall conductivity κ_{HQ}/T. The L-shaped white region in Fig. 3(a) for crystal I resembles that previously reported by Bruin *et al.* [7]. The white region runs vertically from 12 K to about 6 K at around 8 T and then continues horizontally from around 7 T to at least 13 T at about 6 K. For crystal II, κ_{xy}/T reaches to κ_{HQ}/T only in the high temperature and high field regime. This behavior is more in line with what is observed by Czajka *et al.* [10].

IV. SUMMARY

In summary, we report the thermal transport properties of two α-$RuCl_3$ crystals with different amounts of stacking disorder introduced by mechanical deformation. Crystal I shows only one magnetic order at around 13 K. Crystal II has smaller amount of stacking disorder and specific heat data show a dominant transition at 7.6 K and two weak anomalies at around 10 and 13 K. No obvious anomaly in the temperature and field dependence of longitudinal thermal conductivity was observed to be associated with the magnetic order around 10 or 13 K. Similar oscillatory features in the field dependence of thermal conductivity were observed in all crystals that show a dominant magnetic order at around 7 K. For crystal I, an L-type shape was observed for the region in temperature-field space in which thermal Hall conductivity κ_{xy}/T is within ±20% of the half quantized thermal Hall conductivity κ_{HQ}/T. κ_{xy}/T for crystal II reaches κ_{HQ}/T only in the high field and high temperature regime. Our observation suggests that the oscillatory feature is an inherent character of the magnetic phase with T_N near 7 K in the presence of high magnetic fields, while the thermal Hall effect depends on the stacking disorder. The presence of a double-peak feature in the thermal Hall resistivity of Crystal II suggests the potential influence of the opening/closing of a magnon gap on the thermal Hall effect.

ACKNOWLEDGMENTS

J.Y. thanks Satoshi Okamoto and Lucas Lindsay for discussions. H.Z., S.N., M.M., and J.Y. were supported by the U.S. Department of Energy, Office of Science, National Quantum Information Science Research Centers, Quantum Science Center. A.M., H.M., B.S., and D.M. were supported by the U.S. Department of Energy, Office of Science, Basic Energy Sciences, Materials Sciences and Engineering Division.

[1] H. Takagi, T. Takayama, G. Jackeli, G. Khaliullin, and S. E. Nagler, Concept and realization of Kitaev quantum spin liquids, Nat. Rev. Phys. **1**, 264 (2019).

[2] M. A. McGuire, Crystal and magnetic structures in layered, transition metal dihalides and trihalides, Crystals **7**, 121 (2017).

[3] K. W. Plumb, J. P. Clancy, L. J. Sandilands, V. V. Shankar, Y. F. Hu, K. S. Burch, H.-Y. Kee, and Y.-J. Kim, α- $RuCl_3$: A spin-orbit assisted Mott insulator on a honeycomb lattice, Phys. Rev. B **90**, 041112(R) (2014).

[4] Y. Kasahara, T. Ohnishi, Y. Mizukami, O. Tanaka, S. Ma, K. Sugii, N. Kurita, H. Tanaka, J. Nasu, Y. Motome *et al.*, Majorana quantization and half-integer thermal quantum Hall effect in a Kitaev spin liquid, Nature (London) **559**, 227 (2018).

[5] T. Yokoi, S. Ma, Y. Kasahara, S. Kasahara, T. Shibauchi, N. Kurita, H. Tanaka, J. Nasu, Y. Motome, C. Hickey *et al.*, Half-integer quantized anomalous thermal Hall effect in the Kitaev material candidate α-$RuCl_3$, Science **373**, 568 (2021).

[6] M. Yamashita, J. Gouchi, Y. Uwatoko, N. Kurita, and H. Tanaka, Sample dependence of half-integer quantized thermal Hall effect in the Kitaev spin-liquid candidate α-$RuCl_3$, Phys. Rev. B **102**, 220404(R) (2020).

[7] J. A. N. Bruin, R. R. Claus, Y. Matsumoto, N. Kurita, H. Tanaka, and H. Takagi, Robustness of the thermal Hall effect close to half-quantization in α-$RuCl_3$, Nat. Phys. **18**, 401 (2022).

[8] R. Hentrich, M. Roslova, A. Isaeva, T. Doert, W. Brenig, B. Büchner, and C. Hess, Large thermal Hall effect in α-$RuCl_3$: Evidence for heat transport by Kitaev-Heisenberg paramagnons, Phys. Rev. B **99**, 085136 (2019).

[9] É. Lefrançois, G. Grissonnanche, J. Baglo, P. Lampen-Kelley, J.-Q. Yan, C. Balz, D. Mandrus, S. E. Nagler, S. Kim, Y.-J. Kim, N. Doiron-Leyraud, and L. Taillefer, Evidence of a phonon Hall effect in the Kitaev spin liquid candidate α-$RuCl_3$, Phys. Rev. X **12**, 021025 (2022).

[10] P. Czajka, T. Gao, M. Hirschberger, P. Lampen-Kelley, A. Banerjee, N. Quirk, D. G. Mandrus, S. E Nagler, and N. P. Ong, Planar thermal Hall effect of topological bosons in the Kitaev magnet α-$RuCl_3$, Nat. Mater. **22**, 36 (2023).

[11] P. Czajka, T. Gao, M. Hirschberger, P. Lampen-Kelley, A. Banerjee, J. Yan, D. G. Mandrus, S. E. Nagler, and N. P. Ong, Oscillations of the thermal conductivity in the spin-liquid state of α-$RuCl_3$, Nat. Phys. **17**, 915 (2021).

[12] J. A. N. Bruin, R. R. Claus, Y. Matsumoto, J. Nuss, S. Laha, B. V. Lotsch, N. Kurita, H. Tanaka, and H. Takagi, Origin of oscillatory structures in the magnetothermal conductivity of the putative Kitaev magnet α-$RuCl_3$, APL Mater. **10**, 090703 (2022).

[13] É. Lefrançois, J. Baglo, Q. Barthélemy, S. Kim, Y.-J. Kim, and L. Taillefer, Oscillations in the magnetothermal conductivity of α-$RuCl_3$: Evidence of transition anomalies, Phys. Rev. B **107**, 064408 (2023).

[14] S. Suetsugu, Y. Ukai, M. Shimomura, M. Kamimura, T. Asaba, Y. Kasahara, N. Kurita, H. Tanaka, T. Shibauchi, J. Nasu *et al.*, Evidence for a phase transition in the quantum spin liquid state of a Kitaev candidate α-$RuCl_3$, J. Phys. Soc. Jpn. **91**, 124703 (2022).

[15] P. Lee, Quantized (or not quantized) thermal Hall effect and oscillations in the thermal conductivity in the Kitaev spin liquid candidate $RuCl_3$, J. Club Condens. Matter Physi. (2021).

[16] Y. Kubota, H. Tanaka, T. Ono, Y. Narumi, and K. Kindo, Successive magnetic phase transitions in α-RuCl$_3$: XY-like frustrated magnet on the honeycomb lattice, Phys. Rev. B **91**, 094422 (2015).

[17] X. Mi, X. Wang, H. Gui, M. Pi, T. Zheng, K. Yang, Y. Gan, P. Wang, A. Li, A. Wang *et al.*, Stacking faults in α-RuCl$_3$ revealed by local electric polarization, Phys. Rev. B **103**, 174413 (2021).

[18] R. D. Johnson, S. C. Williams, A. A. Haghighirad, J. Singleton, V. Zapf, P. Manuel, I. I. Mazin, Y. Li, H. O. Jeschke, R. Valentí, and R. Coldea, Monoclinic crystal structure of α-RuCl$_3$ and the zigzag antiferromagnetic ground state, Phys. Rev. B **92**, 235119 (2015).

[19] H. B. Cao, A. Banerjee, J.-Q. Yan, C. A. Bridges, M. D. Lumsden, D. G. Mandrus, D. A. Tennant, B. C. Chakoumakos, and S. E. Nagler, Low-temperature crystal and magnetic structure of α-RuCl$_3$, Phys. Rev. B **93**, 134423 (2016).

[20] J.-Q. Yan, B. C. Sales, M. A. Susner, and M. A. McGuire, Flux growth in a horizontal configuration: An analog to vapor transport growth, Phys. Rev. Mater. **1**, 023402 (2017).

[21] J.-Q. Yan and M. A. McGuire, Self-selecting vapor growth of transition-metal-halide single crystals, Phys. Rev. Mater. **7**, 013401 (2023).

[22] R. Hentrich, A. U. B. Wolter, X. Zotos, W. Brenig, D. Nowak, A. Isaeva, T. Doert, A. Banerjee, P. Lampen-Kelley, D. G. Mandrus, S. E. Nagler, J. Sears, Y. J. Kim, B. Büchner, and C. Hess, Unusual phonon heat transport in α-RuCl$_3$: Strong spin-phonon scattering and field-induced spin gap, Phys. Rev. Lett. **120**, 117204 (2018).

[23] D. Hirobe, M. Sato, Y. Shiomi, H. Tanaka, and E. Saitoh, Magnetic thermal conductivity far above the Néel temperature in the Kitaev-Magnet candidate α-RuCl$_3$, Phys. Rev. B **95**, 241112(R) (2017).

[24] I. A. Leahy, C. A. Pocs, P. E. Siegfried, D. Graf, S.-H. Do, K.-Y. Choi, B. Normand, and M. Lee, Anomalous thermal conductivity and magnetic torque response in the honeycomb magnet α-RuCl$_3$, Phys. Rev. Lett. **118**, 187203 (2017).

[25] Y. Kasahara, S. Suetsugu, T. Asaba, S. Kasahara, T. Shibauchi, N. Kurita, H. Tanaka, and Y. Matsuda, Quantized and unquantized thermal Hall conductance of the Kitaev spin liquid candidate α-RuCl$_3$, Phys. Rev. B **106**, L060410 (2022).

[26] See Supplemental Material at http://link.aps.org/supplemental/10.1103/PhysRevMaterials.7.114403 for (1) oscillatory features reported in literature, (2) thermal conductivity of 2%-Ir doped RuCl$_3$, (3) psudocolor plot of thermal Hall conductivity scaled by sample temperature for crystal I, and (4) scaled thermal Hall conductivity data used in Figs. 3(b) and 3(d).